SAND2017-6454C

Time-Domain Analysis of Power System Stability with Damping Control and Asymmetric Feedback Delays

David A. Copp, Felipe Wilches-Bernal, Ian Gravagne, and David A. Schoenwald

***Abstract*—Power systems can be stabilized using distributed control methods with wide-area measurements for feedback. However, wide-area measurements are subject to time delays in communication, which can have undesirable effects on system performance. We present time-domain analysis results regarding the small-signal stability of a two-area power system with damping control subjected to asymmetric time delays in the feedback measurements. We consider two wide-area damping control implementations. The first is implemented with a High Voltage DC transmission line, and the second uses distributed Energy Storage devices. Numerical results show regions of stability for the closed-loop systems that depend on the time delays and the choice of the control gain. These results show that increasing the control gains cause the systems to be less robust to time delays, and, under certain conditions, increasing the time delays can have a stabilizing effect. Furthermore, we provide analysis of time simulations and eigenvalue plots that verify these stability regions and show how stability is affected as time delays increase.**

I. Introduction

A power system consists of a complex interconnection of nonlinear components distributed across wide geographic regions, and these regions may have sparse concentrations of power loads and generation distributed between them. In these systems, sudden increases or decreases in load or generation result in swings in the power transfer between regions. These power swings are called inter-area oscillations [1], and they occur in the western North American Power System (wNAPS) and around the world. Damping inter-area oscillations is crucial for maintaining a secure and reliable power grid, and failing to do so can have severe consequences, such as the blackouts experienced throughout the wNAPS in 1996 [2].

Traditionally, Power System Stabilizers (PSSs), utilizing local measurements, have been used to implement damping control that mitigates the effects of inter-area oscillations. More recently, the use of remote signals with PSSs has been shown to be advantageous [3]. System-wide information has been used in damping control implemented with distributed resources, system components such as Thyristor Controlled Series Compensators (TCSCs), energy storage, and renewable resources [4]–[7]. Additionally, implementing damping control with High Voltage DC (HVDC) transmission lines has been proposed and successfully implemented [8], [9].

D. Copp, F. Wilches-Bernal, and D. Schoenwald are with Sandia National Laboratories, Albuquerque, NM (e-mail: dcopp@sandia.gov). Ian Gravagne is with the Electrical & Computer Engineering Department at Baylor University, Waco, TX. Sandia National Laboratories is a multi-mission laboratory managed and operated by National Technology and Engineering Solutions of Sandia, LLC., a wholly owned subsidiary of Honeywell International, Inc., for the U.S. Department of Energy's National Nuclear Security Administration under contract DE-NA-0003525.

Although system-wide information may enable and improve the performance of damping controllers, the latencies associated with remote signals can have unexpected and detrimental effects on system performance. This paper investigates the effects that asymmetric delays in feedback signals have on the stability of a two-area power system that is prone to inter-area oscillations. Two different implementations of a wide-area damping controller are considered, where power injections in each area of the power system are computed using wide-area information. These two control implementations are based on a controllable HVDC transmission line and on distributed Energy Storage (ES) devices. Without delays, the two control implementations are identical; however, the presence of asymmetric delays causes the closed-loop dynamics to be different and affects system stability and performance.

Several techniques have been used for studying small-signal stability of power systems subject to time delays. In [10], the effect of asymmetric network latencies are analyzed using time-domain simulations as well as root locus methods and computing the maximum singular value of the input sensitivity function. However, only an HVDC-based damping controller is considered. In other work [11], we apply a Lyapunov-Krasovskii approach to determine delay-dependent sufficient conditions for stability of a power system with damping control and asymmetric time delays.

In this work, we perform time-domain simulations to analyze the closed-loop stability of an example two-area power system prone to inter-area oscillations. From these simulations, we determine regions of stability that depend on the size of the time delays and the choice of the control gain for both closed-loop systems with HVDC and ES based damping controllers. The results show that increasing the control gain causes each system to be less robust to time delays, but increasing the time delays may stabilize each system. The phenomenon that delayed feedback can stabilize a system has been documented previously for oscillatory systems with positive feedback [12]. Furthermore, we analyze the movement of the poles of the closed-loop systems as the time delays increase.

This paper is organized as follows. We first introduce power system dynamics and damping controllers in Section II. Next we present numerical results for a representative two-area power system in Section III. Finally, Section IV contains concluding remarks and directions for future work.

II. Problem Formulation

A. Two-Area Power System Model

Power system inter-area phenomena can be analyzed using low order models. These models are usually the result of aggregating multiple generators using coherency-based methods [13], [14]. The dynamics of interest for small-signal stability can be obtained from the linearization of a system where generators are represented by electromechanical models. In this paper, we consider the two-area power system shown in Figure 1, which has one generator per area and a dominant inter-area oscillation.

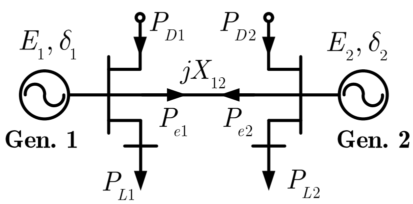

Fig. 1. A two-area power system represented with one generator in each area.

The electromechanical model for the synchronous generators in Figure 1 is given as in [13], for $i = 1, 2$, by

$$\begin{aligned} \dot{\delta}_i &= \Omega\omega_i \\ 2H_i\dot{\omega}_i &= P_{mi} - P_{ei} - D_i\omega_i - \frac{1}{R_i}\omega_i - P_{Li} + P_{Di} \end{aligned} \tag{1}$$

with the power flow between the areas given by

$$P_{e1} = C_{12}\sin(\delta_1 - \delta_2), \qquad P_{e2} = C_{21}\sin(\delta_2 - \delta_1).$$

The states of the system are the generators' rotor angles δ_i and angular velocities ω_i, for $i = 1, 2$. The scalars C_{12} and C_{21} are given by $C_{12} = X_{12}^{-1}E_1E_2$ and $C_{21} = X_{12}^{-1}E_2E_1$, respectively, where X_{12} is the impedance (assumed to be only reactive) of the transmission line connecting the two areas, and E_1 and E_2 are the internal voltage angles of generators 1 and 2, respectively. The parameter Ω is the per-unit constant used for unit conversion. The aggregated load and controllable power injection in the i^{th} area are denoted by P_{Li} and P_{Di}, respectively. P_{mi} represents the mechanical power input to the i^{th} machine, and D_i denotes its damping. The governing droop constant of area i is denoted by R_i.

A linearized model for system (1) can be used in order to study its small-signal stability. A block diagram of the linear model is given in Figure 2, where

$$G_i(s) = \frac{1}{2H_is + D_i},$$

and H_i is the inertia constant of machine i. In this model, we assume the reference signals Δr_1 and Δr_2 are equal to zero.

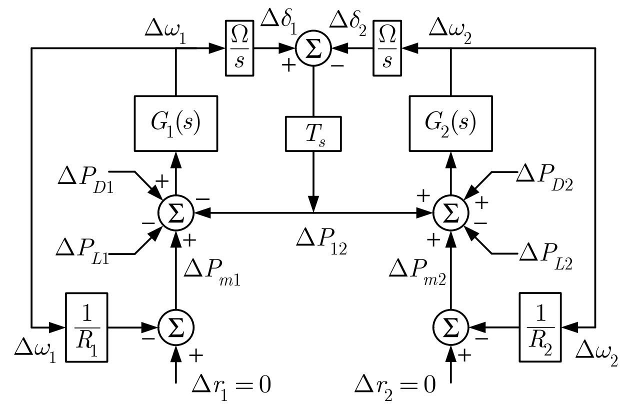

Fig. 2. Block diagram for the linear model of a two-area power system (adapted from [1]).

Defining the state of the linearized system as $x(t) = [\Delta\delta(t)^\top \;\; \Delta\omega(t)^\top]^\top$, where $\Delta\delta(t) = [\Delta\delta_1(t) \quad \Delta\delta_2(t)]^\top$ is the vector of generator rotor angles and $\Delta\omega(t) = [\Delta\omega_1(t) \;\; \Delta\omega_2(t)]^\top$ is the vector of generator angular velocities, the linear dynamics for the two-area power system in Figure 2 can be written as

$$\dot{x}(t) = Ax(t) + B_DP_D(t) + B_LP_L(t). \tag{2}$$

The system A matrix is given by

$$A = \begin{bmatrix} \mathbf{0} & \Omega I \\ -(2H)^{-1}T_s & -(2H)^{-1}(D + R^{-1}) \end{bmatrix},$$

where $\mathbf{0}$ denotes a matrix with appropriate dimensions and all elements equal to zero, and I denotes the identity matrix. The matrix,

$$T_s = \begin{bmatrix} -C_{12}\cos(\bar{\delta}_1 - \bar{\delta}_2) & C_{12}\cos(\bar{\delta}_1 - \bar{\delta}_2) \\ C_{21}\cos(\bar{\delta}_2 - \bar{\delta}_1) & -C_{21}\cos(\bar{\delta}_2 - \bar{\delta}_1) \end{bmatrix}$$

is the synchronizing torque matrix that has a Laplacian structure. Parameters $\bar{\delta}_1$ and $\bar{\delta}_2$ denote the operating conditions (at which the system is linearized) of the rotor angles of the generators in Areas 1 and 2, respectively. The matrices D, R, and H are defined as

$$D = \begin{bmatrix} D_1 & 0 \\ 0 & D_2 \end{bmatrix}, \quad R = \begin{bmatrix} R_1 & 0 \\ 0 & R_2 \end{bmatrix}, \quad H = \begin{bmatrix} H_1 & 0 \\ 0 & H_2 \end{bmatrix}.$$

The input matrices for the power injections $P_D(t) = [P_{D1}(t) \quad P_{D2}(t)]^\top$ and aggregated loads $P_L(t) = [P_{L1}(t) \;\; P_{L2}(t)]^\top$ are given by

$$B_D = \begin{bmatrix} \mathbf{0} \\ (2H)^{-1} \end{bmatrix}, \qquad B_L = -B_D.$$

(Open-loop) stability of the linear system (2) can be determined by computing the eigenvalues of the system A matrix. For this two-area system, the A matrix has four eigenvalues. Due to the Laplacian nature of matrix T_s, one of the eigenvalues is at the origin, and because the damping and droop coefficients D_i and R_i, respectively, are positive, the remaining three eigenvalues lie in the left-half plane. Therefore, system (2) is (open-loop) stable. Next we present two implementations of a damping controller and later investigate the stability of the resulting closed-loop system.

B. Damping Control

In this section, we present a damping controller that is designed to compute power injection inputs $P_D(t)$ in order to improve the damping of system (2). As previously mentioned, we are interested in the small-signal stability of power systems that are prone to inter-area oscillations. These types of systems have a pair of eigenvalues with low damping (i.e., they are close to the imaginary axis). The objective of a damping controller is to increase the damping of this pair of eigenvalues (i.e., move them further into the left half plane). We consider a damping controller of the form

$$P_D(t) = \begin{bmatrix}\mathbf{0} & K\end{bmatrix} x(t), \tag{3}$$

where K is a gain matrix given by

$$K = \begin{bmatrix} -k_d & k_d \\ k_d & -k_d \end{bmatrix},$$

and k_d is the control gain to be selected. The resulting power injections $P_{D1}(t)$ and $P_{D2}(t)$ have the same magnitude but opposite sign. This type of damping controller was proposed for the wNAPS in [8] and has since been successfully implemented and tested [9].

Now we can rewrite the system (2) as

$$\dot{x}(t) = A_{cl}x(t) + B_L P_L(t), \tag{4}$$

where

$$A_{cl} = \begin{bmatrix} \mathbf{0} & \Omega I \\ -(2H)^{-1}T_s & -(2H)^{-1}(D + R^{-1} - K) \end{bmatrix}.$$

The stability of the resulting closed-loop system (4) can be analyzed by computing the eigenvalues of the matrix A_{cl}.

C. Delay in the Feedback Signals

The control architecture considered here is often called wide-area damping control because the measurement devices and control resources are widely distributed across large geographic areas. Wide-area damping control has been made possible due to the deployment of Phasor Measurement Unit (PMU) technology that allows for, e.g., voltage and frequency measurements to be collected throughout the power system [15]. Because of this architecture, the feedback measurements must be communicated over a network using, for instance, internet protocols and are, therefore, subject to time delays. In this section, we present two different implementations of the damping controller (3) and discuss how they differ when subjected to time delays in the feedback signals. We assume that the generator angular velocities $\Delta\omega(t)$ are measured and available for feedback.

A depiction of a two-area power system is shown in Figure 3, where two measurements are taken (one in each area). These measurements are transmitted to the controllers in each area, which compute the power injections that increase damping in the system. Each measurement is subject to a time delay. In this work, we assume that there are only two (asymmetric) delays and that they are constant. The first delay τ_1 occurs when transmitting the local measurement, i.e., the measurement in Area 1 to the controller in Area 1 and likewise for Area 2. The second delay τ_2 occurs when transmitting the remote measurements, i.e., the measurement in Area 1 from the controller in Area 1 to the controller in Area 2 and likewise for Area 2. Although it may be natural to assume that local measurement delays are smaller than remote measurement delays, for full generality, we make no assumptions about the size of the delays. In practice, these delays depend on the communication channels linking the controller and the remote measurement devices.

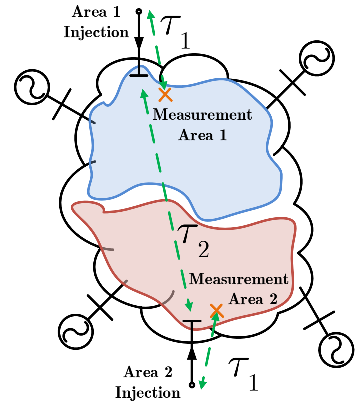

Fig. 3. Power injections and measurement delays in a two-area power system.

1) Damping Control using HVDC: A controllable HVDC transmission line may be used to implement the controller (3). In this implementation, there is just a single controller located in either area, and the injection in the area without the controller is simply the negative of the power injection implemented by the controller (assuming no losses), i.e., $P_{D1}(t) = -P_{D2}(t)$. Incorporating the local and inter-area time delays τ_1 and τ_2, as shown in Figure 3, and neglecting losses, the HVDC damping controller is given by

$$\begin{aligned} P_{D1}(t) &= -k_d(\Delta\omega_1(t-\tau_1) - \Delta\omega_2(t-\tau_2)) \\ P_{D2}(t) &= k_d(\Delta\omega_1(t-\tau_1) - \Delta\omega_2(t-\tau_2)), \end{aligned} \tag{5}$$

and the closed-loop system is given by the following linear Delay Differential Equation (DDE)

$$\dot{x}(t) = Ax(t) + A_1^{\mathrm{HV}}x(t-\tau_1) + A_2^{\mathrm{HV}}x(t-\tau_2) + B_L P_L(t), \tag{6}$$

where

$$A_1^{\mathrm{HV}} = \begin{bmatrix} 0 & 0 & 0 & 0 \\ 0 & 0 & 0 & 0 \\ 0 & 0 & \frac{-k_d}{2H_1} & 0 \\ 0 & 0 & \frac{k_d}{2H_2} & 0 \end{bmatrix}, \; A_2^{\mathrm{HV}} = \begin{bmatrix} 0 & 0 & 0 & 0 \\ 0 & 0 & 0 & 0 \\ 0 & 0 & 0 & \frac{k_d}{2H_1} \\ 0 & 0 & 0 & \frac{-k_d}{2H_2} \end{bmatrix}.$$

2) Damping Control using Energy Storage: Instead of using an HVDC transmission line, one could install an ES device co-located with a controller in each area to provide power injections. In this case, each controller is subject to a local and inter-area time delay, as shown in Figure 3. Then the ES enabled damping controllers are given by

$$\begin{aligned} P_{D1}(t) &= -k_d(\Delta\omega_1(t-\tau_1) - \Delta\omega_2(t-\tau_2)) \\ P_{D2}(t) &= k_d(\Delta\omega_1(t-\tau_2) - \Delta\omega_2(t-\tau_1)), \end{aligned} \tag{7}$$

and the closed-loop system is given by the following DDE

$$\dot{x}(t) = Ax(t) + A_1^{\text{ES}}x(t-\tau_1) + A_2^{\text{ES}}x(t-\tau_2) + B_L P_L(t), \quad (8)$$

where

$$A_1^{\text{ES}} = \begin{bmatrix} 0 & 0 & 0 & 0 \\ 0 & 0 & 0 & 0 \\ 0 & 0 & \frac{-k_d}{2H_1} & 0 \\ 0 & 0 & 0 & \frac{-k_d}{2H_2} \end{bmatrix}, \; A_2^{\text{ES}} = \begin{bmatrix} 0 & 0 & 0 & 0 \\ 0 & 0 & 0 & 0 \\ 0 & 0 & 0 & \frac{k_d}{2H_1} \\ 0 & 0 & \frac{k_d}{2H_2} & 0 \end{bmatrix}.$$

The differences between the closed-loop dynamics for the HVDC system (6) and the ES system (8) appear in the matrices A_1^{ES}, A_1^{HV} and A_2^{ES}, A_2^{HV}.

III. Time-Domain Stability Analysis

In this Section we present numerical results analyzing the stability of the two-area power system in Figure 2 for both damping control implementations subjected to asymmetric time delays in the feedback signals. We assume that the two areas are identical with the following parameter values: $D_1 + R_1^{-1} = D_2 + R_2^{-1} = 0.1$, $H_1 = H_2 = 5/2$, and $T_s = 14$. With these parameter values, the open-loop system (i.e., $k_d = 0$) has a complex pair of eigenvalues located at $-0.01 \pm 2.336j$, which corresponds to the inter-area mode of the system.

A. Time Simulations

Thirty second time simulations of the HVDC system (6) and the ES system (8) are performed for several values of the control gain k_d and time delays from zero to nine seconds. Although nine second time delays may be impractically large, we consider them here in order to show the resulting structure that appears in the delay-dependent regions of stability. After one second, a unit step input in the aggregated load in Area 1, ΔP_{L1}, is applied, resulting in inter-area oscillations.

The objective of a damping controller is to effectively damp the response of the system after a fault. Physically, this means driving the angular velocities of the generators to the same value more quickly than would naturally occur. Therefore, closed-loop stability and performance can be quantified by computing $|\Delta\omega_1(t) - \Delta\omega_2(t)|$. If this quantity decreases over time, the system is stable. The faster the quantity decreases, the better the damping performance. Our stability criterion is given precisely in Figure 4. The resulting stability regions are shown in Figure 5. As the control gain k_d is increased, the closed-loop systems are stable for fewer values of the time delays. Furthermore, the unstable regions also grow as the time delays increase.

Due to the oscillatory nature of the system response, delayed measurements may still be fairly accurate as long as the delays are close to an integer multiple of the period of oscillation. The undamped oscillation for this example (shown in Figure 4) has a frequency of 0.367 Hz. Therefore, the period of oscillation is about 2.73 seconds, and when the delays are 1.36 seconds, the measurements are π radians out of phase with the true state. Looking at Figure 5(a), delays that are odd integer multiples of 1.36 seconds lead to injections that destabilize the system, whereas delays that are integer multiples of 2.73 seconds lead to injections that preserve stability of the system. Therefore, increasing one or both time delays to better match the period of oscillation may be beneficial. However, this is not necessarily the case as the control gain is increased, as

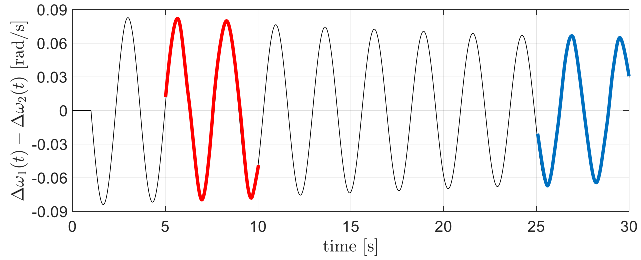

Fig. 4. Stability criterion. If the largest amplitude of the response between 5 and 10 seconds (red) is larger than the largest amplitude of the response between 25 and 30 seconds (blue), the system is declared to be stable. Otherwise, the system is unstable. This is the response of system (2) with no control (i.e., $P_D(t) = 0$ for all t), and it is stable.

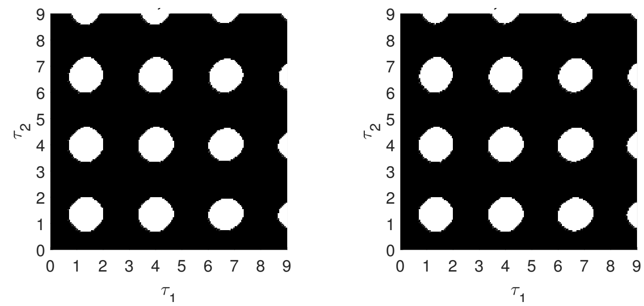

(a) $k_d = 0.1$

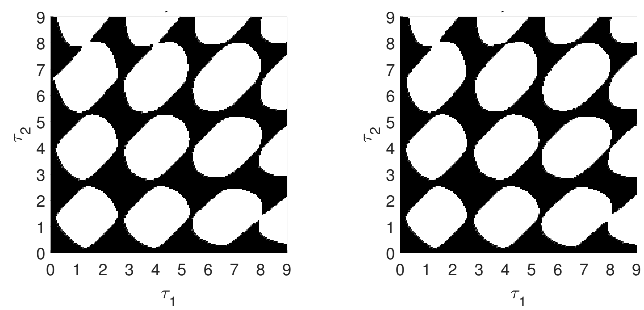

(b) $k_d = 1$

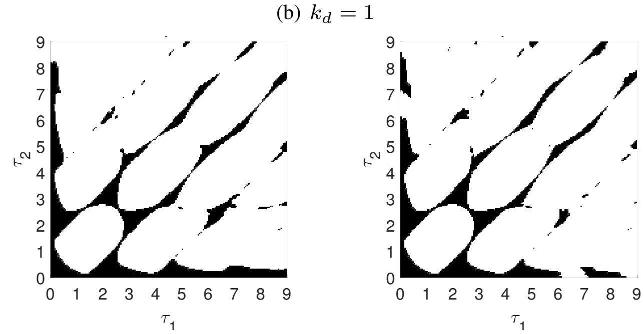

(c) $k_d = 3$

Fig. 5. Regions of stability (black areas) for the HVDC system (6) (left) and the ES system (8) (right) for several values of control gain k_d.

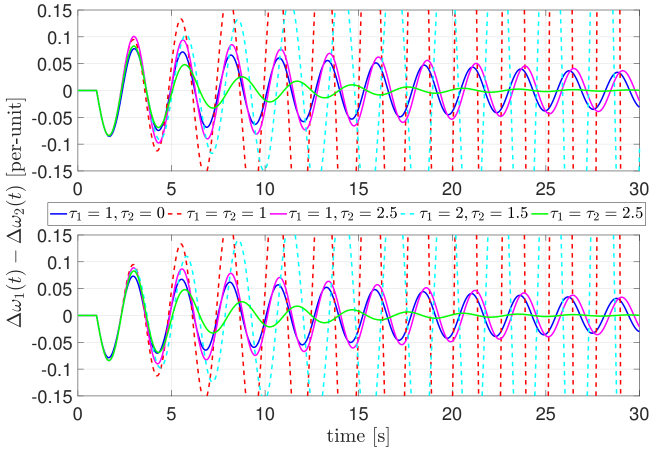

Fig. 6. Responses of the HVDC system (6) (top) and ES system (8) (bottom) with $k_d = 1$ and several values for the time delays. Increasing one or both of the time delays can stabilize the system.

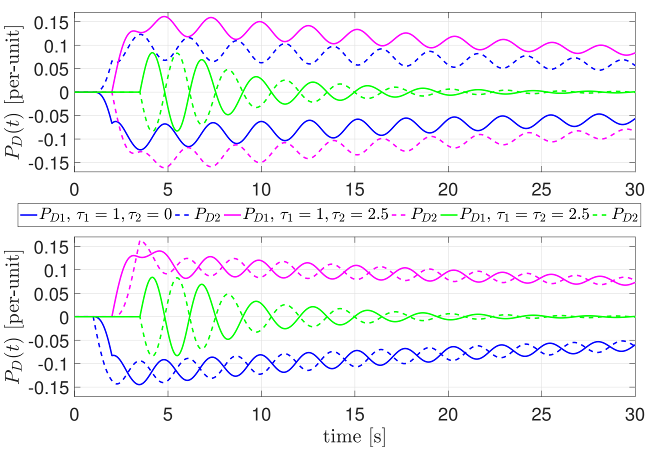

Fig. 7. Power injections $P_D(t)$ for the HVDC system (6) (top) and ES system (8) (bottom) with $k_d = 1$ and several values for the time delays. These injections correspond to the stable responses shown in Figure 6. Solid and dashed lines represent injections in Area 1 and Area 2, respectively.

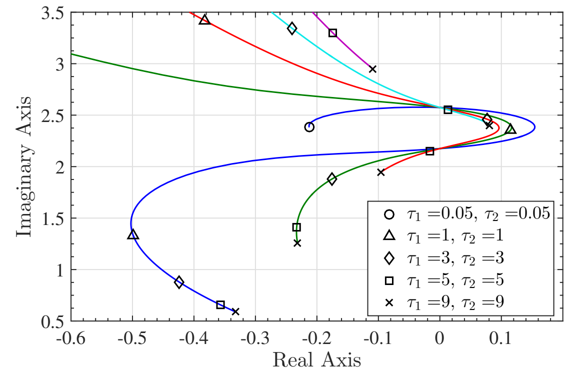

(a) HVDC and ES with equal time delays and $k_d = 1$

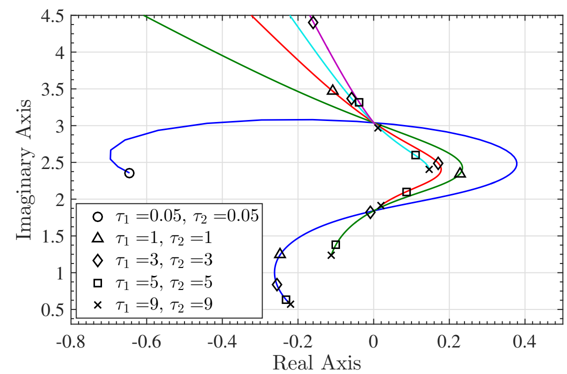

(b) HVDC and ES with equal time delays and $k_d = 3$

Fig. 8. Poles of both the HVDC and ES systems (6) and (8) as the time delays increase and are equal. Each colored line indicates motion of an individual pole as the values of the time delays change, and symbols indicate the location of the poles for particular values of the time delays.

in Figures 5(b) and 5(c). Larger control gains amplify the effects of errors in the feedback measurements, so smaller errors can lead to injections that destabilize the systems. This relationship between oscillation frequency and time delays leading to instability is ongoing work.

Figure 6 shows simulations for both the HVDC and ES systems for several values of time delays and $k_d = 1$. When the time delays are equal to $\tau_1 = \tau_2 = 1$, both systems are unstable. However, if τ_1 is kept the same and τ_2 is increased to 2.5, both systems are stable. Therefore, increasing the time delays may stabilize the systems. The power injections $P_D(t)$ resulting in the stable responses in Figure 6 are shown in Figure 7. As expected, the injections from the HVDC based damping controller (5) are symmetric about 0, and when the time delays are equal, $\tau_1 = \tau_2 = 2.5$, the two damping controllers are identical. When the time delays are asymmetric, the injections from the controllers (5) and (7) are different.

B. Eigenvalue Analysis

To further analyze these systems, we next present figures plotting the poles (equivalently, the eigenvalues) of the closed-loop systems and show how they move as the time delays increase. Because the HVDC and ES systems (6) and (8), respectively, have an infinite number of poles, we first approximate both systems using a Padé approximation of sufficiently high order (in this case, 37 was chosen) to show all of the relevant poles (near the imaginary axis).

Figures 8-9 show how the poles that cross the imaginary axis move as the time delays are increased for different values of the control gain k_d. These are zoomed-in plots that neither show the symmetric eigenvalues below the real axis that exhibit the same behavior nor the poles on the real axis that never cross into the right-half-plane. In these figures, it is clear that the HVDC and ES systems are different; for instance, the ES system has more poles close to the imaginary axis. Interestingly, for a particular system, all of the poles that cross the imaginary axis cross in the same locations. However, as the value of the control gain k_d increases, the poles that cross into the right-half-plane move farther to the right. This corresponds to the system being unstable for more values of the time delays, as is seen in Figure 5. Therefore, the systems are less robust to time delays as the control gain is increased.

IV. Conclusion

We investigated the small-signal stability of a representative two-area power system that is prone to inter-area oscillations. Two wide-area damping control implementations subjected to time delays in their feedback signals were considered. We presented regions where the closed-loop systems are stable depending on the size of the time delays and the chosen control gain. Increasing the control gain causes the systems to be less robust to time delays, but increasing the time delays may have a stabilizing effect. Moreover, we showed how the eigenvalues of the closed-loop systems move as the time delays increase.

Future work will investigate the advantages and disadvantages of each damping controller implementation, regarding transient performance and magnitude of the control actions.

V. Acknowledgment

Funding for this research was provided by the US DOE Energy Storage Program managed by Dr. Imre Gyuk of the DOE Office of Electricity Delivery and Energy Reliability.

References

[1] P. Kundur, *Power System Stability and Control*. New York, NY: McGraw-Hill, 1994.

[2] D. N. Kosterev, C. W. Taylor, and W. Mittelstadt, "Model validation for the August 10, 1996 WSCC system outage," *IEEE Trans. Power Syst.*, vol. 14, no. 3, pp. 967–979, Aug. 1999.

[3] J. H. Chow, J. J. Sanchez-Gasca, H. Ren, and S. Wang, "Power system damping controller design using multiple input signals," *IEEE Control Syst. Mag.*, vol. 20, no. 4, pp. 82–90, Aug. 2000.

[4] A. Chakrabortty, "Wide-area damping control of power systems using dynamic clustering and TCSC-based redesigns," *IEEE Trans. Smart Grid*, vol. 3, no. 3, pp. 1503–1514, Sept. 2012.

[5] F. Dörfler, M. R. Jovanović, M. Chertkov, and F. Bullo, "Sparsity-promoting optimal wide-area control of power networks," *IEEE Transactions on Power Systems*, vol. 29, no. 5, pp. 2281–2291, Feb. 2014.

[6] J. Neely, R. Byrne, R. Elliott, C. Silva-Monroy, D. Schoenwald, D. Trudnowski, and M. Donnelly, "Damping of inter-area oscillations using energy storage," in *Power and Energy Soc. General Meeting, IEEE*, Vancouver, BC, 2013, pp. 1–5.

[7] F. Wilches-Bernal, C. Lackner, and J. H. Chow, "Power system controllability through nontraditional generation," in *Conf. on Decision and Control (CDC), IEEE*, Las Vegas, NV, 2016, pp. 702–708.

[8] D. Trudnowski, D. Kosterev, and J. Undrill, "PDCI damping control analysis for the western North American power system," in *Power and Energy Soc. General Meeting, IEEE*, Vancouver, BC, 2013, pp. 1–5.

[9] D. Trudnowski, B. Pierre, F. Wilches-Bernal, D. Schoenwald, R. Elliott, J. Neely, R. Byrne, and D. Kosterev, "Initial closed-loop testing results for the Pacific DC Intertie wide area damping controller," in *Power and Energy Soc. General Meeting, IEEE*, Chicago, IL, 2017, pp. 1–5.

[10] F. Wilches-Bernal, R. Concepcion, J. C. Neely, D. A. Schoenwald, R. H. Byrne, B. J. Pierre, and R. T. Elliott, "Effect of time delay asymmetries in power system damping control," in *Power and Energy Soc. General Meeting, IEEE*, Chicago, IL, 2017, pp. 1–5.

[11] F. Wilches-Bernal, D. A. Copp, I. Gravagne, and D. A. Schoenwald, "Stability criteria for power systems with damping control and asymmetric feedback delays," Submitted, 2017.

[12] C. Abdallah, P. Dorato, J. Benites-Read, and R. Byrne, "Delayed positive feedback can stabilize oscillatory systems," in *Proc. of the American Control Conference*, 1993, pp. 3106–3107.

[13] J. H. Chow, *Power System Coherency and Model Reduction*. New York, NY: Springer, 2013.

[14] D. Romeres, F. Dörfler, and F. Bullo, "Novel results on slow coherency in consensus and power networks," in *2013 European Control Conference (ECC)*, Zurich, Switzerland, 2013, pp. 742–747.

[15] A. Chakrabortty and P. P. Khargonekar, "Introduction to wide-area control of power systems," in *American Control Conference (ACC)*. IEEE, 2013, pp. 6758–6770.

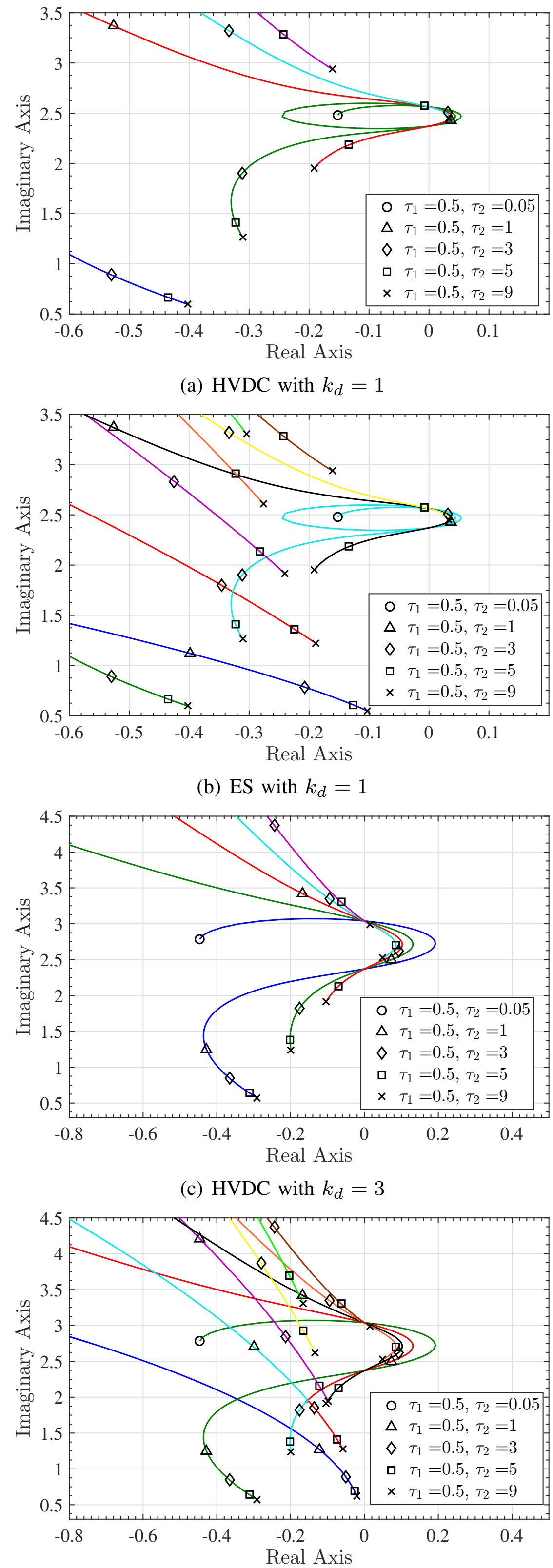

(a) HVDC with $k_d = 1$

(b) ES with $k_d = 1$

(c) HVDC with $k_d = 3$

(d) ES with $k_d = 3$

Fig. 9. Poles of HVDC system (6) and ES system (8) with $\tau_1 = 0.5$ and τ_2 increasing from 0.5 to 9. Each colored line indicates motion of an individual pole as the values of the time delays change, and symbols indicate the location of the poles for particular values of the time delays.